

# Application of finite difference method for solving problem of seismic resistance of underground pipelines

*Rakhmatjon Khusainov*<sup>1,2\*</sup>, *Javlon Yarashov*<sup>2</sup>, and *Saparboy Khusainov*<sup>3, 4</sup>

<sup>1</sup>Institute of Mechanics and Seismic Stability of Structures of the Academy of Sciences of the Republic of Uzbekistan, Tashkent, Uzbekistan

<sup>2</sup>Tashkent Institute of Irrigation and Agricultural Mechanization Engineers"" National Research University, Tashkent, Uzbekistan

<sup>3</sup>Bauman Moscow State Technical University, Moscow, Russia

<sup>4</sup>Tashkent State Transport University, Tashkent, Uzbekistan

**Abstract.** The paper analyzes the dynamic response of an underground main pipe under the action of a longitudinal wave propagating in soil along the pipe. The article assumes that the elastic pipe is of a finite length, and a linear viscoelastic model of the "pipe-soil" system interaction is considered. The problem is solved numerically using the explicit scheme of the finite difference method. A longitudinal wave in the soil is taken as a traveling sine wave. The article presents a comparative analysis of the results for certain values of elastic and viscous interaction coefficients, propagation velocity, and pulse duration. Under elastic interaction of the "pipe-soil" system, the reflection of the wave propagating in the underground pipeline at the boundaries of the pipeline coincides with the propagating wave in soil, leading to an increase in the maximum deformation of the underground pipeline, the value of which can double. The viscosity coefficient of interaction at the "pipe-soil" system contact leads to attenuation of the wavefront in the underground pipeline. For soils with values of viscous interaction coefficient of more than 100 kN·s/m<sup>2</sup>, this may lead to complete attenuation of the bursts at the wavefront in the pipeline. The choice of the step ratio in coordinate and time equal to the wave propagation velocity in the pipeline allows for obtaining results that coincide with the exact solution.

## 1 Introduction

Underground pipelines are a key component of critical life support systems such as water supply, gas and liquid fuels, sewerage, electricity, and telecommunications. The interaction with the soil structure caused by seismic waves has an important effect on pipeline behavior, and the integration across the entire pipeline network affects the entire system's performance [1, 2].

In recent decades, much attention has been paid to the impact of wave propagation on

---

\*Corresponding author: [r.khusainov89@yandex.com](mailto:r.khusainov89@yandex.com)

segmented underground pipelines. In [2-6], various models were proposed to analyze the interaction of segmented pipelines during wave propagation.

Damage to underground pipelines during an earthquake could be caused by various hazards: permanent soil deformation (landslides, liquefaction, and seismic settlement) and wave propagation effect. The latter is characterized by transient deformation and ground curvature caused by the traveling wave effect. A simple procedure considering one traveling wave with an undamped (traveling) waveform was proposed by T.R. Rashidov and N.M. Newmark [7, 8] to analyze the wave propagation. According to T.R. Rashidov's statement, the static theory was first considered by R.M. Mukurdumov [9] and then given in the monograph by Sh.G. Napetvaridze [10], where he proposed that during wave propagation along the pipeline, the pipe and the soil move in the same way. N.M. Newmark later proposed a similar assumption that the underground pipeline strictly follows the soil movement, called a static theory. Therefore, the maximum axial deformation of the pipe is the same as the maximum axial deformation of soil.

However, the above procedures consider infinite pipe lengths and therefore do not consider their effective length and construction work (constraint conditions). In [11], analytical relationships were developed for a pipe of finite length subjected to various combinations of boundary conditions (i.e., free end, fixed or elastic end) for pipelines of different lengths. In 1962, T.R. Rashidov proposed a differential equation for an underground pipeline, which became the basis of the T.R. Rashidov's dynamic theory [7, 11]. G. De Martino et al. [12] and V. Corrado et al. [13] developed models of the pipe-soil interaction, taking into account the finite length of the pipeline. Assuming a linear elastic model of soil motion and ignoring the slip at the pipe-soil contact interface, the model analyzes the dynamic behavior of a finite-length pipeline considering the boundary conditions at the ends. It was assumed that the pipeline was continuous; that is, any fluctuations between the characteristics (parameters) of the pipeline and its joints were considered insignificant. A.A. Ilyushin and T.R. Rashidov [2] proposed a visco-elastoplastic model of the underground structure interaction with the soil.

In works [14-24], different mechanical and mathematical models were analyzed, and several urgent problems of underground and ground structures were solved.

The effect of the coefficients of elasticity, viscosity, and plasticity of the pipeline interaction with soil on the stress-strain state of an underground pipeline is studied in detail in [25-30]. In [13, 29], the influence of inertial forces on the deformed state of an underground pipeline was studied in detail. Accumulated experience demonstrates that direct simulation of real objects in the general case is not ensuring the required quality of the relevant analytical models [31].

Let us consider the problem of longitudinal vibration of an underground main pipeline under linear viscoelastic interaction at the contact with soil, with three types of fastening [25].

$$m \cdot \frac{\partial^2 u}{\partial t^2} - E \cdot F \cdot \frac{\partial^2 u}{\partial x^2} + \pi \cdot D \cdot \frac{\mu}{H} \cdot \left( \frac{\partial u}{\partial t} - \frac{\partial u_g}{\partial t} \right) + \pi \cdot D \cdot k_x \cdot (u - u_g) = 0 \quad (1)$$

here  $m$  is the weight per unit length of the pipeline;  $E$  is Young's modulus of the pipe material;  $F$  is the cross-sectional area of the underground pipeline;  $k_x$  is the coefficient of elastic interaction of the "pipe-soil" system [2];  $\mu$  is the coefficient of viscous interaction of the "pipe-soil" system, that is, the resistance of the equivalent velocity of the interaction of the "pipe-soil" system;  $H$  is the laying depth;  $D$  is the outer diameter of the underground pipeline;  $u(x,t)$  is the absolute displacement in the section  $x$  of the

underground pipeline at the point in time  $t$ ;  $u_g(x, t)$  is the ground displacement corresponding to the section  $x$  of the underground pipeline at the point in time  $t$ .

In addition, ground motion can be represented as an impulse: a half-sine wave, triangle, or trapezoid. Ground displacement parallel to the pipe can be written as

$$u_g = \begin{cases} A \cdot \sin \omega(t - x/C_p), & \text{if } t > x/C_p, \\ 0, & \text{if } t \leq x/C_p, \end{cases} \quad (2)$$

where  $A$  – is the maximum soil displacement;  $\omega$  – is the angular velocity of seismic wave vibration determined by the formula  $\omega = 2\pi/T$ ;  $C_p$  – is the "apparent velocity" of wave propagation (hereinafter referred to as the wave propagation velocity in soil). The "apparent velocity" of wave propagation in the soil can be greater due to the wave's angle of incidence to the pipeline axis or due to the flexible joints of the pipeline.

Ground motion is written in strains:

$$\varepsilon_g = \begin{cases} -(A/C_p) \cdot \cos \omega(t - x/C_p), & \text{if } t > x/C_p, \\ 0, & \text{if } t \leq x/C_p. \end{cases} \quad (3)$$

If an underground pipeline is pliantly fixed at the ends, then the boundary conditions are taken in the following form

$$\begin{aligned} EF \frac{\partial u}{\partial x} &= k_{N1}(u - u_g), \quad \text{for } x=0, t > 0, \\ EF \frac{\partial u}{\partial x} &= -k_{N2}(u - u_g), \quad \text{for } x=L, t > 0. \end{aligned} \quad (4)$$

Where  $k_{N1}$ ,  $k_{N2}$  are the coefficients of compliance of the fastening at the left and right ends of the underground pipeline.

## 2 Methods

The study in [25] compares the methods of Crank-Nicholson, McCormack, and Courant-Friedrich-Lewy (explicit scheme). It shows the accuracy of the explicit scheme relative to other methods when solving discontinuous problems of vibrations of underground pipelines. In this study, the problem is solved by the finite difference method in an explicit scheme. Careful numerical calculations are performed to prevent unwanted vibrations near the discontinuity (deformation wavefront).

The problem is solved using an explicit finite-difference scheme; Courant's conditions must be satisfied to obtain results that coincide with the exact solution. It was shown in [25] that the choice of the step ratio in coordinate and time in the form (5) for problem (1) allows one to obtain results that coincide with the exact solution.

$$\Delta x / \Delta t = a, \quad (6)$$

where  $a = \sqrt{E \cdot F / m}$  is the wave propagation velocity in the pipeline. We pass to dimensionless variables according to the following formulas:

$$\bar{x} = x / a = x / \sqrt{EF / K}, \quad \bar{t} = t / b = t / \sqrt{m / K}, \quad \bar{u} = u / A, \quad \bar{u}_g = u_g / A. \quad (6)$$

Here  $K = \pi \cdot D \cdot k_x$ ;  $M = (\pi \cdot D \cdot \mu) / H$ ;  $c = M / (K \cdot b)$ .

With (6), we rewrite equation (1) in the form

$$\frac{\partial^2 \bar{u}}{\partial \bar{t}^2} - \frac{\partial^2 \bar{u}}{\partial \bar{x}^2} + c \cdot \frac{\partial \bar{u}}{\partial \bar{t}} + \bar{u} = c \cdot \frac{\partial \bar{u}_g}{\partial \bar{t}} + \bar{u}_g \quad (7)$$

where the ground motion  $\bar{u}_g$  is given as

$$\bar{u}_g = \begin{cases} \sin \omega (b \bar{t} - a \bar{x} / C_p), & \text{if } b \bar{t} > a \bar{x} / C_p, \\ 0, & \text{if } b \bar{t} \leq a \bar{x} / C_p. \end{cases} \quad (8)$$

Elastically fixed boundary conditions are:

$$a) \quad \left. \frac{E \cdot F}{a} \cdot \frac{\partial \bar{u}}{\partial \bar{x}} \right|_{\bar{x}=0} = k_{N1} \cdot (\bar{u} - \bar{u}_g) \Big|_{\bar{x}=0} \quad b) \quad \left. \frac{E \cdot F}{a} \cdot \frac{\partial \bar{u}}{\partial \bar{x}} \right|_{\bar{x}=L/a} = -k_{N2} \cdot (\bar{u} - \bar{u}_g) \Big|_{\bar{x}=L/a} \quad (9)$$

To solve equation (8), the method of finite differences of the second order of accuracy is used:

$$\frac{\partial^2 \bar{u}}{\partial \bar{t}^2} \approx \frac{\bar{u}_i^{j+1} - 2\bar{u}_i^j + \bar{u}_i^{j-1}}{\Delta \bar{t}^2}, \quad \frac{\partial^2 \bar{u}}{\partial \bar{x}^2} \approx \frac{\bar{u}_{i+1}^j - 2\bar{u}_i^j + \bar{u}_{i-1}^j}{\Delta \bar{x}^2} \quad (11)$$

$$\frac{\partial \bar{u}}{\partial \bar{t}} \approx \frac{\bar{u}_i^{j+1} - \bar{u}_i^{j-1}}{2 \cdot \Delta \bar{t}}, \quad \frac{\partial \bar{u}_g}{\partial \bar{t}} \approx \frac{\bar{u}_{gi}^{j+1} - \bar{u}_{gi}^{j-1}}{2 \cdot \Delta \bar{t}} \quad (12)$$

$$\bar{u} \approx \frac{\bar{u}_i^{j+1} + 2\bar{u}_i^j + \bar{u}_i^{j-1}}{4}, \quad \bar{u}_g \approx \frac{\bar{u}_{gi}^{j+1} + 2\bar{u}_{gi}^j + \bar{u}_{gi}^{j-1}}{4} \quad (13)$$

Let us substitute the approximations of the differentials of the function in time and coordinate (11) and (12) and the displacement function (13) into the differential equation (8), obtaining

$$\bar{u}_i^{j+1} = (b_6 \cdot (\bar{u}_{i+1}^j + \bar{u}_{i-1}^j) - b_3 \cdot \bar{u}_i^j - b_2 \cdot \bar{u}_i^{j-1} + b_4 \cdot (\bar{u}_{gi}^{j+1} - \bar{u}_{gi}^{j-1}) + b_5 \cdot (\bar{u}_{gi}^{j+1} + 2 \cdot \bar{u}_{gi}^j + \bar{u}_{gi}^{j-1})) / b_1. \quad (14)$$

Where,

$$b_1 = 1 + c \Delta t / 2 + \Delta t^2 / 4; \quad b_2 = 1 - c \Delta t / 2 + \Delta t^2 / 4; \quad b_3 = 2 \Delta t^2 / \Delta x^2 + \Delta t^2 / 2 - 2;$$

$$b_4 = c \cdot \Delta t / 2; \quad b_5 = \Delta t^2 / 4; \quad b_6 = \Delta t^2 / \Delta x^2.$$

$$\bar{t} = \Delta \bar{t} \cdot j, \quad \bar{x} = \Delta \bar{x} \cdot i. \quad (15)$$

(9) is written using (15)

$$\bar{u}_{gi}^j = \begin{cases} \sin \omega(b \cdot \Delta \bar{t} \cdot j - (a \cdot \Delta \bar{x} \cdot i) / C_p), & \text{if } b \cdot \Delta \bar{t} \cdot j > (a \cdot \Delta \bar{x} \cdot i) / C_p, \\ 0, & \text{if } b \cdot \Delta \bar{t} \cdot j \leq (a \cdot \Delta \bar{x} \cdot i) / C_p. \end{cases} \quad (16)$$

Consider both ends of an elastically fixed underground pipeline with boundary conditions (10), a and b. Let us approximate the boundary conditions:

$$\begin{aligned} \text{a) } & \frac{E \cdot F}{a} \cdot \frac{(-3 \cdot \bar{u}_0^j + 4 \cdot \bar{u}_1^j - \bar{u}_2^j)}{2 \cdot \Delta \bar{x}} = \frac{k_{N1}}{4} \cdot (\bar{u}_0^{j+1} + 2 \cdot \bar{u}_0^j + \bar{u}_0^{j-1} - \bar{u}_{g0}^{j+1} - 2 \cdot \bar{u}_{g0}^j - \bar{u}_{g0}^{j-1}), \\ \text{b) } & \frac{E \cdot F}{a} \cdot \frac{\bar{u}_{N-2}^j - 4 \cdot \bar{u}_{N-1}^j + 3 \cdot \bar{u}_N^j}{2 \cdot \Delta \bar{x}} = -\frac{k_{N2}}{4} \cdot (\bar{u}_N^{j+1} + 2 \cdot \bar{u}_N^j + \bar{u}_N^{j-1} - \bar{u}_{gN}^{j+1} - 2 \cdot \bar{u}_{gN}^j - \bar{u}_{gN}^{j-1}). \end{aligned} \quad (17)$$

Then, for  $j = 0$  we have

$$\bar{u}_0^1 = (-2\bar{u}_0^0 + \bar{u}_{g0}^1 + 2\bar{u}_{g0}^0 + \bar{u}_{g0}^{-1}) / 2 \quad \text{and} \quad \bar{u}_N^1 = (-2\bar{u}_N^0 + \bar{u}_{gN}^1 + 2\bar{u}_{gN}^0 + \bar{u}_{gN}^{-1}) / 2$$

for  $j > 0$ :

$$\begin{aligned} \text{a) } & \bar{u}_0^{j+1} = \frac{2 \cdot E \cdot F}{a \cdot \Delta \bar{x} \cdot k_{N1}} \cdot (-3 \cdot \bar{u}_0^j + 4 \cdot \bar{u}_1^j - \bar{u}_2^j) - 2 \cdot \bar{u}_0^j - \bar{u}_0^{j-1} + \bar{u}_{g0}^{j+1} + 2 \cdot \bar{u}_{g0}^j + \bar{u}_{g0}^{j-1}, \\ \text{b) } & \bar{u}_N^{j+1} = -\frac{2 \cdot E \cdot F}{a \cdot \Delta \bar{x} \cdot k_{N2}} \cdot (\bar{u}_{N-2}^j - 4 \cdot \bar{u}_{N-1}^j + 3 \cdot \bar{u}_N^j) - 2 \cdot \bar{u}_N^j - \bar{u}_N^{j-1} + \bar{u}_{gN}^{j+1} + 2 \cdot \bar{u}_{gN}^j + \bar{u}_{gN}^{j-1}. \end{aligned} \quad (18)$$

The following system of equations is solved

$$\begin{cases} \bar{u}_0^{j+1} = \frac{2 \cdot E \cdot F}{a \cdot \Delta \bar{x} \cdot k_{N1}} \cdot (-3 \cdot \bar{u}_0^j + 4 \cdot \bar{u}_1^j - \bar{u}_2^j) - 2 \cdot \bar{u}_0^j - \bar{u}_0^{j-1} + \bar{u}_{g0}^{j+1} + 2 \cdot \bar{u}_{g0}^j + \bar{u}_{g0}^{j-1}, \\ \bar{u}_i^{j+1} = [b_6 \cdot (\bar{u}_{i+1}^j + \bar{u}_{i-1}^j) - b_3 \cdot \bar{u}_i^j - b_2 \cdot \bar{u}_i^{j-1} + b_4 \cdot (\bar{u}_{gi}^{j+1} - \bar{u}_{gi}^{j-1}) + \\ + b_5 \cdot (\bar{u}_{gi}^{j+1} + 2 \cdot \bar{u}_{gi}^j + \bar{u}_{gi}^{j-1})] / b_1, \quad 0 < i < N, \\ \bar{u}_N^{j+1} = -\frac{2 \cdot E \cdot F}{a \cdot \Delta \bar{x} \cdot k_{N2}} \cdot (\bar{u}_{N-2}^j - 4 \cdot \bar{u}_{N-1}^j + 3 \cdot \bar{u}_N^j) - 2 \cdot \bar{u}_N^j - \bar{u}_N^{j-1} + \bar{u}_{gN}^{j+1} + 2 \cdot \bar{u}_{gN}^j + \bar{u}_{gN}^{j-1}. \end{cases} \quad (19)$$

After solving the system of algebraic equations (19), we determine the displacements in dimensionless form.

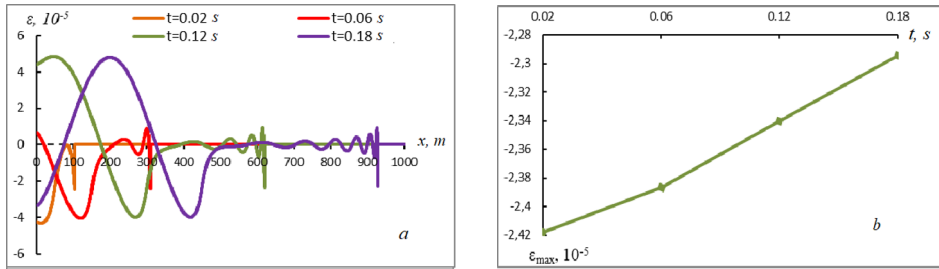
Steel pipe characteristics are modulus of elasticity  $E = 2.1 \cdot 10^{11} \text{ N/m}^2$ , outer diameter  $D = 0.61 \text{ m}$ , thickness  $s = 0.01 \text{ m}$ , mass per unit length  $m = 141.1 \text{ kg/m}$ ,  $k_{N1} = k_{N2} = 29 \cdot 10^4 \text{ kN/m}$ .

Soil characteristics are elastic interaction coefficient  $k_x = 0.5 \cdot 10^4 \text{ kN/m}^3$ , viscous interaction coefficient  $\mu = 100 \text{ kN} \cdot \text{s/m}^2$ , wave propagation velocity  $C_p = 2500 \text{ m/s}$ , harmonic wave period  $T = 0.2 \text{ s}$ , and wave amplitude  $A = 0.004 \text{ m}$ .

### 3 Results and discussion

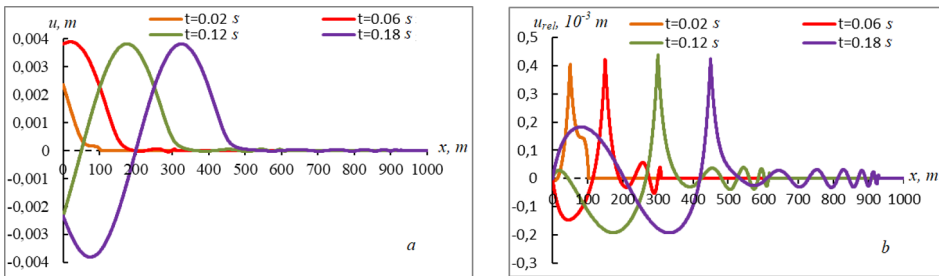
The wave propagation in a steel pipeline is 5120 m/s, and in the soil, this velocity depends on soil type. Let us assume that a wave in soil moves with an apparent velocity of 2500 m/s.

Fig. 1 shows the change in the deformation of an underground main pipeline of a length of 1 km along the coordinate, both ends of which are fixed in the ground. From Fig. 1, a, it can be seen that at times  $t = 0.02$  s,  $t = 0.06$  s,  $t = 0.12$  s, and  $t = 0.18$  s, the wavefront in the pipeline reaches distances of 103.3, 309.8, 619.6, and 929.3 m, respectively. The maximum deformation at the wavefront in the pipeline is approximately two times less than the maximum deformation in soil. Figs. 1, a, and b show the change in the deformation of the underground pipeline along the coordinate under elastic interaction  $k_x = 0.5 \times 10^7$  N/m<sup>3</sup>. It was found that with the wave propagation through an underground pipeline over time, the amplitude of oscillations at the wavefront in an underground pipeline slowly decreases. Before the front wave arrival at 929.4 m, the amplitude at the wavefront decreases by about 5.7%. This is the phenomenon of the wavefront attenuation in a pipe with a zero coefficient of viscous resistance, which appeared due to an error in the computational scheme.



**Fig. 1.** Change in underground pipeline deformation along the coordinate (a) and wavefront deformation of underground pipeline (b) at times  $t = 0.02, 0.06, 0.12,$  and  $0.18$  s

Fig. 2 shows the change in the absolute (a) and relative (b) displacements of the underground pipeline along the coordinate for the points in time 0.02, 0.06, 0.12, and 0.18 s.



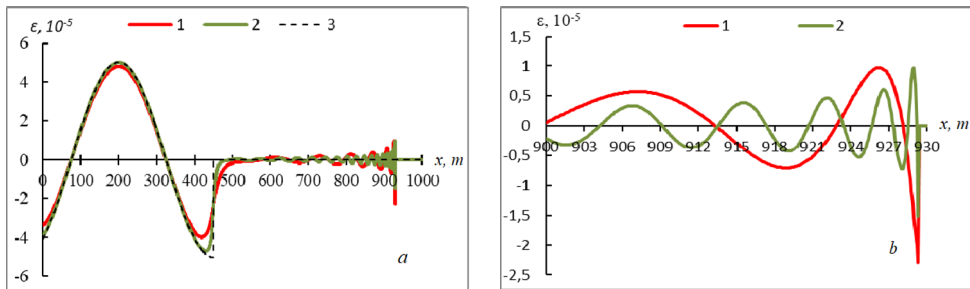
**Fig. 2.** Change in absolute (a) and relative (b) displacements of underground pipeline along coordinate

As seen from Fig. 3, a, the wavefront in soil reaches the 450th-meter point at  $t = 0.18$  s from the left end, with an increase in the coefficient of elasticity of interaction  $k_x$  from  $0.5 \times 10^4$  to  $4.5 \times 10^4$  kN / m<sup>3</sup>, the deformation of the underground pipeline approaches to the value of soil deformation. Fig. 3, b shows the change in deformation behind the wavefront in the pipeline at a value of the elastic interaction coefficient of  $0.5 \times 10^7$  and  $4 \times 10^7$  N /

m<sup>3</sup>. It can be seen here that the coefficient of elastic interaction affects not only the frequency of oscillations behind the wavefront of the pipeline but also the amplitude of deformation at the front of the pipeline.

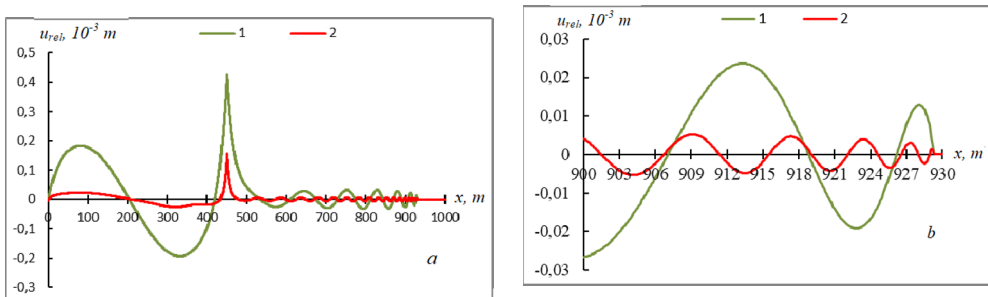
With an increase in the coefficient of elastic interaction, the value of the pipeline deformation at the wavefront decreases, and the oscillation frequency behind the pipeline wavefront increases. Immediately behind the wavefront in the pipeline, the soil resists so that the deformation at a certain distance behind the front changes sign, and gradually, with distance from the wavefront, the deformation oscillations damp out. At the same time, the wave in the soil propagates through the lateral surface of the pipeline and excites a wave in the pipeline.

Here, with an increase in the value of the elastic resistance of soil, the frequency of oscillations behind the front increases.



**Fig. 3.** Change in deformation of underground main pipeline along the coordinate with elastic properties of "pipe-soil" system interaction at  $t = 0.18$  s: 1 –  $k_x = 0.5 \cdot 10^7$  N / m<sup>3</sup>; 2 –  $k_x = 4 \cdot 10^7$  N / m<sup>3</sup>; 3 - wave in soil

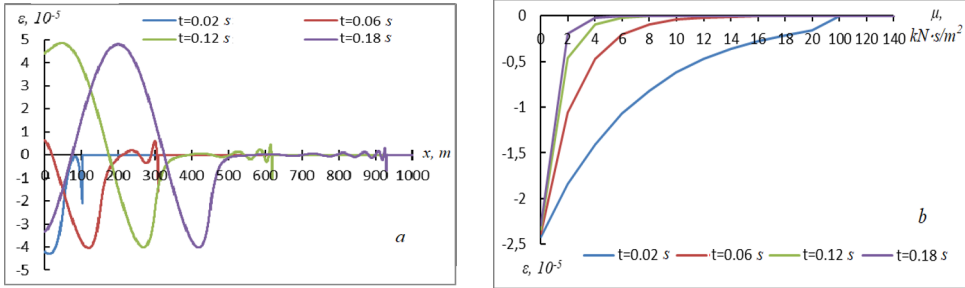
Fig. 4 shows the change in relative displacements along the length of the underground main pipeline; the interaction between the pipeline and the ground is considered elastic. It can be seen here that the relative displacement reaches its maximum value at the wavefront in the soil. At  $t = 0.18$  s, the wave reaches the 450th meter of a 1000 m long underground pipeline. With an increase in the coefficient of elastic resistance, the maximum value of the relative displacement greatly decreases. Behind the wavefront of the pipeline, high-frequency oscillations appear, the amplitude of which increases with distance. Fig. 4b shows the influence of the value of elastic resistance on the amplitude of oscillation of the relative displacement behind the wavefront in the pipeline.



**Fig. 4.** Change of relative displacements along coordinate at  $t = 0.18$ s and  $\mu = 0$ , N·s/m<sup>2</sup>: 1 –  $k_x = 0.5 \cdot 10^7$  N / m<sup>3</sup>; 2 –  $k_x = 4 \cdot 10^7$  N / m<sup>3</sup>

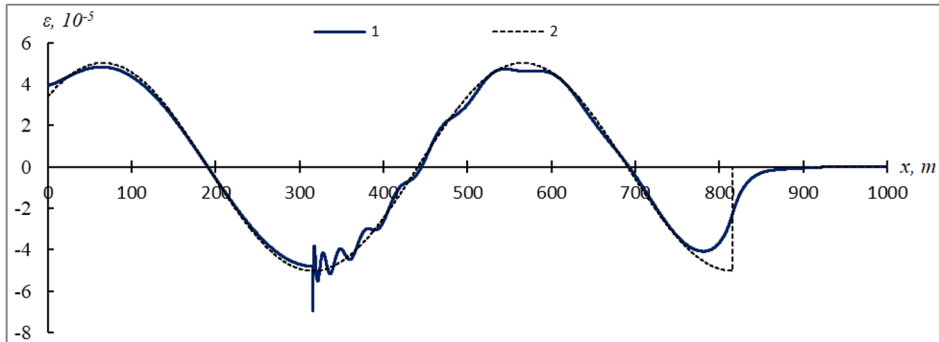
Figure 5, a, shows the change in the underground main pipeline with visco-elastic interaction properties. As seen, with distance, the amplitude at the wavefront in the pipeline

strongly decreases due to the viscosity of the interaction. Fig. 5, b shows a graph of the change in deformation at the wavefront in the pipeline according to the coefficient of viscosity of the interaction for four points in time. At viscous resistance values greater than 100 kN·s/m<sup>2</sup>, the maximum value at the wavefront greatly decreases and is approximately zero (see Fig. 5, b).



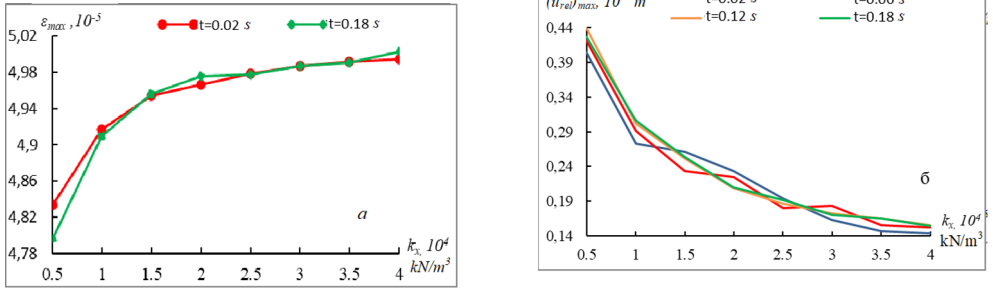
**Fig. 5.** Change in the deformation of an underground pipeline along the coordinate  $\mu = 1 \text{ kN}\cdot\text{s}/\text{m}^2$ ,  $k_x = 0.5 \cdot 10^7 \text{ N}/\text{m}^3$

Figure 6 shows the case in which the reflected wavefront at the rigidly fixed end of the pipeline coincides with the wavefront in the pipeline. When these waves coincide, the maximum deformation value in the underground pipeline increases up to one and a half times. In Fig. 6, the maximum deformation value in the underground pipeline is one and a half times less than the maximum deformation in soil. This is due to the presence of the viscosity of the interaction and the error of the numerical scheme. To determine the time of the maximum value of the pipeline deformation, we use the following formula  $t=(2L+T\cdot C_p)/(C_p+a)$  and obtain  $t = 0.32625 \text{ s}$ .



**Fig. 6.** Change in deformation of underground pipeline along the coordinate, at  $\mu = 1 \text{ kN}\cdot\text{s} / \text{m}^2$ ,  $k_x = 0.5 \cdot 10^7 \text{ N} / \text{m}^3$ ,  $t=(2L+T\cdot C_p)/(C_p+a)$ ,  $t = 0.32625 \text{ s}$ .





**Fig. 7.** Change in maximum value of deformation (a) and relative displacement (b) according to coefficient of elastic interaction at contact

Figure 7 shows the change in the maximum deformation in terms of the coefficient of elastic interaction for the points in time 0.12 and 0.18 s. Hence, it can be seen that with an increase in the coefficient of elastic interaction, the maximum deformation value in the underground pipeline tends to be the maximum value of deformation in soil.

Figure 7b shows the maximum values of the relative displacement for different values of the coefficient of elastic interaction. As established, with an increase in the coefficient of elastic interaction from  $0.5 \times 10^4$  to  $4 \times 10^4$  kN / m<sup>3</sup>, the maximum relative displacement decreases threefold.

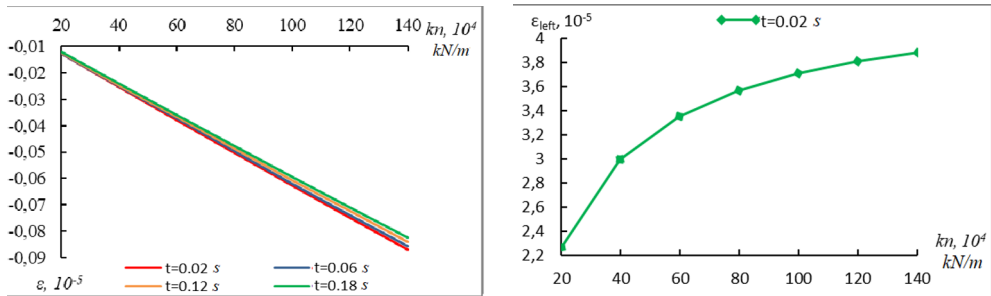


**Fig. 8.** Change in deformation at wavefront in pipeline according to coefficient of elastic fastening of ends of underground main pipeline

**Fig. 9.** Change in deformation at left end according to coefficient of elastic fastening of the ends of underground main pipeline

Now consider an underground main pipeline when both ends are elastically anchored in the ground. The elastic fixing coefficients are denoted by  $kn_1$  and  $kn_2$ . Let us assume that the coefficients of elastic interaction  $kn_1$  and  $kn_2$  are equal to each other and equal to  $kn$ . Fig. 8 shows the influence of the compliance coefficient of fastenings on the deformation values at the wavefront in an underground main pipeline. With an increase in the fixing compliance coefficient, the deformation values at the wavefront increase linearly. It was found that the compliance coefficient affects the deformation values at the compliantly attached boundaries (Fig. 9).

### 4 Conclusions

When the ground moves in the form of a traveling sine wave, an underground pipeline undergoes deformations close to the deformation in soil. An increase in the elastic coefficient of interaction leads to an increase in deformation in the buried pipeline.

The reflection of the wavefront at the fixed end increases the deformation of the underground pipeline by approximately one and a half times.

The compliance coefficient was found to affect the deformation values at the compliantly attached boundaries.

The viscosity coefficient of the interaction contributes to the attenuation of the wavefront, depending on the value of the coefficient.

## References

1. Rourke T.D. Geohazards and large geographically distributed systems. -p 503-543, 2010.
2. Rashidov T. Dynamic theory of seismic stability of complex systems of underground structures. - Tashkent: Fan, 180 p. 1973.
3. Rourke M.J. and Liu X. Response of buried pipelines subject to earthquake effects. MCEER Monograph 3, Multidisciplinary Center for Earthquake Engineering Research, University at Buffalo, Buffalo, NY, USA, 1999.
4. Iwamoto T., Wakai N., Yamaji T. Observation of dynamic behavior of ductile iron pipelines during earthquakes.: Proceedings of the 8th World Conference on Earthquake Engineering, Vol. VII. San Francisco, USA; p. 231-238, 1984. O'Rourke T.D., Wang Y., Shi P. Advances in lifeline earthquake engineering.: Proceedings of the 13th World Conference on Earthquake Engineering, Vancouver, Canada; Paper No. 5003, 2004.
5. Wang LRL. Some aspects of seismic resistant design of buried pipelines.: Lifeline earthquake engineering: buried pipelines, seismic risk, and instrumentation (PVP-34). American Society of Mechanical Engineers; p. 117-131, 1979.
6. Rashidov T. Differential Equation of Oscillation of an Underground Pipeline during an Earthquake., Reports of the Academy of Sciences of the UzSSR, No. 9. - P.10-12, 1962.
7. Newmark N.M. "Problems in wave propagation in soil and rocks," in Proceedings of the International Symposium on Wave Propagation and Dynamic Properties of Earth Materials, University of New Mexico Press. pp. 7-26, 1967.
8. Mukurdumov R.M. Seismic resistance of underground pipelines.. AN UzSSR, 1953.
9. Napetvaridze Sh.G. Seismic resistance of hydraulic structures. M., Gosstroyizdat, 216 p. 1959.
10. Rashidov T. Calculation of underground pipelines of finite length for the impact of a short-term seismic load. Tashkent, Reports of the Academy of Sciences UzSSR, No.4, p.13-16, 1963.
11. De Martino G., D'Acunto B., Fontana N., and Giugni M. Dynamic response of continuous buried pipes in seismic areas, in ASCE Pipelines Conference, August 2006.
12. Corrado V., D'Acunto B., Fontana N., and Giugni M. Inertial Effects on Finite Length Pipe Seismic Response.. P.14, 2012.
13. Abirov, R.A., Khusanov, B.E., and Sagdullaeva, D.A. Numerical modeling of the problem of indentation of elastic and elastic-plastic massive bodies. Conf. Ser.: Mater. Sci. Eng. 971 032017, 2020.
14. Mirsaidov, M.M., Sultanov, T.Z., Yarashov, J.A. Strength of earth dams considering elastic-plastic properties of soil. Magazine of Civil Engineering. 108(8). Article No. 10813, 2021. DOI: 10.34910/MCE.108.13
15. Sultanov, K.S., Kumakov, J.X., Loginov, P.V., Rikhsieva, B.B Strength of

- underground pipelines under seismic effects. Magazine of Civil Engineering, 93(1), p.97–120. 2020. <https://doi.org/10.18720/MCE.93.9>
16. Mirsaidov, M.M., and Sultanov, T.Z. Assessment of stress-strain state of earth dams with allowance for non-linear strain of material and large strains Mag. Civ. Eng. (49), p.73–82, 2014.
  17. Sultanov, K. S.and Vatin, N. I. Wave Theory of Seismic Resistance of Underground Pipelines, Appl. Sci. 11, no. 4: 1797, 2021. <https://doi.org/10.3390/app11041797>
  18. Sayapin, S.N., Shkapov, P.M. Application of Baushinger effect during prolonged storage in stressed state of elements of structures made of fiber reinforced plastic. Journal of Physics: Conference Series, 1301(1), 012014, 2019.
  19. Sultanov, K., Khusanov, B. and Rikhsieva, B. Underground pipeline strength under non-one-dimensional motion. IOP Conference Series: Materials Science and Engineering 883 (1), 012023, 2020.
  20. Sultanov, K., Loginov, P., Ismoilova, S., Salikhova, Z. Wave processes in determining mechanical characteristics of soils E3S Web of Conferences, 2019, 97, 04009
  21. Safarov, I., and et al. Vibrations of multilayer composite viscoelastic curved pipe under internal pressure. IOP Conference Series: Materials Science and Engineering, 2021, 1030(1), 012073
  22. Mirsaidov, M., Safarov, I., Teshaev, M., Nuriddinov, B. Eigenwaves propagation in three-layer cylindrical viscoelastic shells with a filler non-uniform in thickness. IOP Conference Series: Materials Science and Engineering, 1030(1), 012074, 2021.
  23. Mirsaidov, M and Usarov, M Bimoment theory construction to assess the stress state of thick orthotropic plates. Conf. Ser.: Earth Environ. Sci. 614 012090, 2020.
  24. Corrado V., D'Acunto B., Fontana N., and Giugni M. Estimation of dynamic strains in finite end- constrained pipes in seismic areas. Mathematical and Computer Modelling, vol.49, № 3-4. p.789-797, 2009.
  25. Khusainov, R.B. Longitudinal Deformation Wave in a Buried Pipeline Subject to Viscoelastic Interaction with Soil. Soil Mech Found Eng 56, p.420–426, 2020.
  26. Khusainov R.B. Behavior of an underground main pipeline under the influence of a traveling impulse in the shape of a triangle. Problems of Computational and Applied Mathematics. №1 (25). p.50-58, 2020.
  27. Rakhmankulova, B., and et al. Underground main pipeline behavior under a travelling impulse in the form of a triangle. International Scientific Conference "Construction Mechanics, Hydraulics and Water Resources Engineerin" (CONMECHYDRO - 2021). E3S Web Conf. Volume 264, 2021. <https://doi.org/10.1051/e3sconf/202126401006>.
  28. Rakhmankulova, B., and et al. Inertia force effect on longitudinal vibrations of underground pipelines. International Scientific Conference "Construction Mechanics, Hydraulics and Water Resources Engineerin" (CONMECHYDRO - 2021). E3S Web Conf. Volume 264, 2021. <https://doi.org/10.1051/e3sconf/202126401007>.
  29. Mirsaidov, M., Sultanov, T., and et al. Estimation of the earth dam strength with inelastic soil properties. IOP Conference Series: Materials Science and Engineering, 883(1), 012021, 2020.
  30. Shkapov, P.M., Sulimov, A.V., Sulimov, V.D. Correction of analytical model for lateral-staging rocket with modal data using hybrid optimization algorithms. AIP Conference Proceedings, 2171, 030013, 2019. <https://doi.org/10.1063/1.5133179>